PCCP

Accepted Manuscript

ROYAL SOCIETY OF CHEMISTRY

www.rsc.org/pccp

ARTICLE TYPE www.rsc.org/xxxxxx | XXXXXXXX

Molecular dynamics simulations of longer *n*-alkanes in silicalite: State-of-the-art models achieving close agreement with experiment

A. J. O'Malley [a, b] **, C.R.A. Catlow** [*a, b]

Received (in XXX, XXX) Xth XXXXXXXXX 200X, Accepted Xth XXXXXXXXX 200X
First published on the web Xth XXXXXXXXX 200X
DOI: 10.1039/b00000000x

The diffusion of longer *n*-alkanes (*n*-C_8 - *n*-C_{16}) in silicalite was studied using molecular dynamics (MD) simulations at a temperature range of 300 - 400 K, with loadings appropriate for direct comparison with previously carried out quasielastic neutron scattering (QENS) studies. The calculated diffusion coefficients were in close agreement with experimental values, significantly closer than those calculated using more primitive framework and hydrocarbon models, and in the case of the longer alkanes, closer agreement than those calculated by MD studies using the same model, but not using experimental loadings. The calculated activation energies of diffusion agreed with experiment to within 1.5 kJ mol^{-1} for shorter alkanes of the range, but with a larger difference for tetra and hexadecane, due to factors which cannot be reproduced using periodic boundary conditions. Channel switching between the straight and sinusoidal channel system was found for octane at higher temperatures, where more than one octane molecule was located in the channel, which was attributed to the molecular size of octane, and the repulsion caused by the presence of the extra octane molecules in the channel system, allowing the potential barrier of channel switching at the junctions to be breached.

Introduction

Due to its relevance to applications in many catalytic conversions, and molecular sieving processes in the petrochemical industry (most notably with the use of ZSM-5, zeolite-X and zeolite-Y),[1] the study of hydrocarbon diffusion in zeolites is of great interest. As the catalytic processes take place within the zeolite channels, the rate limiting steps could be found in either the diffusion of the hydrocarbon toward the active site, or the diffusion of the products away from it. Separation processes also rely on differences in the diffusion coefficients of the components.

A significant amount of work both theoretical and experimental has been carried out studying the diffusion of hydrocarbons in the MFI zeolite structure [2-15], the framework type of industrially important ZSM-5 and its siliceous analogue silicalite. The diffusion of *n*-alkanes longer than octane in this framework is of considerable interest and has been studied by quasi-elastic neutron scattering (QENS) techniques in both Na-ZSM-5[16] and silicalite.[17] The range of *n*-alkanes C_8 - C_{20} has also been studied with hierarchical simulations,[18] and molecular dynamics (MD) simulations.[19, 25]

Earlier molecular dynamics simulations[19] were found to give diffusion coefficients at 300 K too large by 2-3 orders of magnitude, giving also a periodic dependence of diffusivity on chain length, supporting the concepts of the "window effect" [20-23] and resonant diffusion. [24] This discrepancy was found later to be due to the use of too simplistic a model, in particular the use of rigid frameworks and a united atom hydrocarbon model. Our recent study [25] used an explicit atom hydrocarbon model with a flexible framework to study *n*-alkanes of length C_8 – C_{20} and found that not only was a monotonic dependence of diffusivity on chain length exhibited when the most sophisticated model was used, but the majority of absolute values of the diffusion coefficient were all within 1 order of magnitude of QENS studies of the same alkanes in silicalite.[17] The authors noted that the simulations were carried out in the limit of infinite dilution, and sorbate-sorbate interactions would be expected to slow diffusion significantly; also, that the simulations were only carried out at 300 K, and a more suitable test of the accuracy of such simulations would be through calculating the activation energy, gauging the variation of diffusion coefficient with temperature.

The following study employs accurate models to perform state of

[a] *University College London, Department of Chemistry, Materials Chemistry, Third Floor, Kathleen Lonsdale Building, Gower Street, London WC1E 6BT, UK. E-mail: c.r.a.catlow@ucl.ac.uk, a.o'malley@ucl.ac.uk*
[b] *UK Catalysis Hub, Research Complex at Harwell, Rutherford Appleton Laboratory, Harwell Oxford, Didcot, Oxfordshire, OX11 0FA, UK.*

the art molecular dynamics simulations of longer *n*-alkanes (C_8, C_{10}, C_{12}, C_{14} and C_{16}) with all-atom potentials and a flexible framework model 300, 350 and 400 K in silicalite in direct comparison with aforementioned QENS studies by Jobic.[17] Diffusion coefficients and the activation energies are calculated using the same experimental loadings, to ensure the model is as comparable as possible. Our results show that this model is capable of producing diffusion coefficients within a factor of 5 of those observed experimentally at all temperatures, and that a close agreement in activation energy along with the experimental trend of activation energy with chain length can be obtained.

Computational Methods

The techniques used are essentially those employed in our earlier study of hydrocarbons in silicalite[25] details of which are now summarised.

Potential Parameters

The silicalite structure was identical to that used and detailed in reference 25, a 2 x 2 x 2 orthorhombic supercell with pnma symmetry.[26] Full ionic charges were assigned to the Si and O atoms of the framework species. The potentials used to describe the flexible zeolite framework were taken from work studying SiO_2[27] widely used for studying silicalites. These include a Buckingham potential to describe Si-O and O-O interactions, along with a harmonic three-body potential to describe the O-Si-O triads. A cut-off distance of 10Å was used.

The hydrocarbon model employed forcefields derived from vibrational data.[28] Each hydrogen atom was assigned a charge of +0.1 au, and the carbon atoms were assigned the appropriate charge to give an overall charge neutral hydrocarbon. The bonds and bond angle vibrations were described by harmonic potentials while the dihedrals were described by a cosine potential. The guest-host interactions were modelled by a Lennard-Jones potential taken from the work of Kiselev et al[29] as were intramolecular sorbate interactions. All zeolite-zeolite, zeolite-sorbate, and sorbate-sorbate interaction parameters are detailed in reference 25. An important future test of these parameters would be to compare with experimental adsorption isotherms obtained for these systems, as these have never been calculated using the flexible framework and all-atom models of this study. This is however, outside the scope of this work.

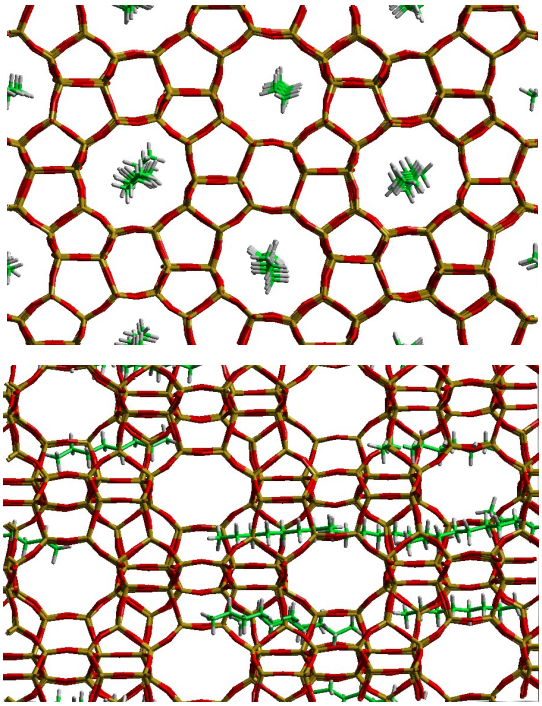

Fig 1. A view of the system for octane pre-production run at 300 K viewed down the (left) [010] direction and (right) [001] direction. All experimental visualisations in this study were created using the visualisation software package Aten1.8.[31]

Simulation Procedure

The alkanes of choice were placed in the centre of the straight channel of the supercell, avoiding strong contact with the channel walls. The straight channel was used as previous QENS studies have shown that *n*-alkanes generally occupy this channel system due to the observation of one dimensional diffusion.[30] The loadings were kept as close as possible to those used in reference 17 (roughly 28 H atoms per unit cell). These loadings corresponded to 1.56 mol/uc for octane, 1.3 mol/uc for decane, 1.08 mol/uc for dodecane, 0.93 mol/uc for tetradecane and 0.82 mol/uc for hexadecane. An example of the starting configuration for the octane MD runs is shown in figure 1.

The system was then equilibrated at the desired temperature for 1 ns in the canonical (NVT) ensemble. After the equilibration run, the production run of 10 ns in the microcanonical (NVE) ensemble was carried out for each alkane set at 300, 350 and 400 K. A timestep of 0.5 fs was used and the atomic coordinates were saved every picosecond (every 2000 steps). A Berendsen[32] thermostat was used to maintain the temperature near a set point, with a time constant for thermal energy exchange set at 1 ps. All simulations were carried out using the DL-POLY-4 code.[33]

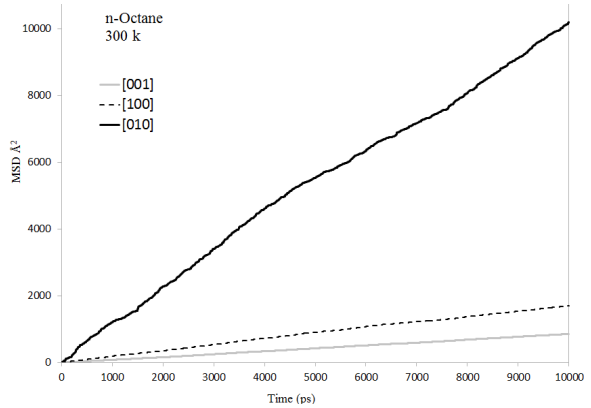

Fig 2. A plot of the mean squared displacement as a function of time for a single *n*-octane molecule at 300 K along the three principle axes of silicalite.

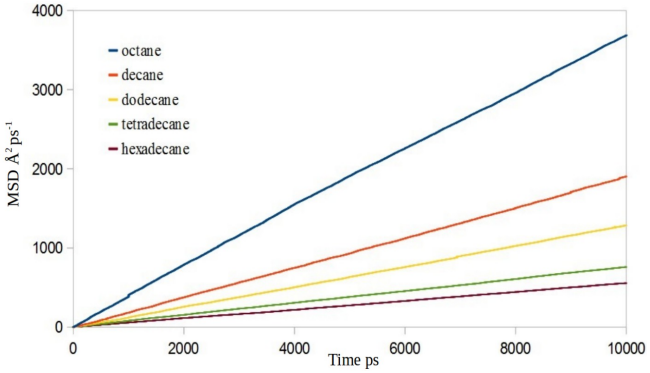

Fig 3. A plot of the average mean squared displacement as a function of time for all alkanes at 300 K in silicalite.

The production time of 10 ns was chosen because it was adequate time to obtain true diffusive motion (illustrated, as discussed below, by a linear mean-squared displacement (MSD). The central carbon atom of each chain then had its coordinates logged, and the average of the mean-squared displacement for all molecules was plotted as shown in figure 3, enabling the self-diffusion coefficients to be calculated from the Einstein relationship:

$$D_s = {}^1/_6 \lim_{t\to\infty} \frac{d}{dt} \langle (\mathbf{r}(t) - \mathbf{r}(0))^2 \rangle , \qquad (1)$$

where the term in braces is the ensemble average of the MSD of the hydrocarbon chain.

Results and Discussion

An important consideration when using the Einstein relationship to calculate a diffusion coefficient is that the simulation time must be long enough to obtain true diffusive motion, i.e. the mean squared displacement must be linear with respect to time over the measured range. As shown for the simulation run of a selected single molecule of *n*-octane in figure 2 and the average mean squared displacement of all molecules in figure 3, this linearity is well achieved. This linearity was confirmed before calculating the diffusion coefficient for each chain length. It is difficult to obtain the statistical errors of these diffusion coefficient values, however the very linear nature of the MSD plots in figure 3 suggests that these errors are very low.

The diffusion coefficients for all chain lengths, at all temperatures are tabulated in table 1, with those calculated at 300 K plotted in figure 4. As expected, the experimentally observed monotonic decrease in diffusion coefficient with chain length was observed. Importantly, all the calculated diffusion coefficients were well within 1 order of magnitude of the QENS measurements. The lowest correlation being with hexadecane at 300 K, differing from QENS studies by a factor of 3.68, which is still a marked improvement on the lowest correlation in reference 25 (hexadecane) which differed by a factor of 26, suggesting that the use of experimental loadings can lower the calculated

Table 3. A comparison of Ds values in $m^2 s^{-1}$ obtained by the current MD simulations, hierarchical simulations[18] and QENS studies[17], for all alkanes at all temperatures.

N	T (K)	Ds (MD)	Ds (QENS)	Ds (HS)	Ds (MD) /Ds (QENS)
8		$6.09\ 10^{-10}$	$2.0\ 10^{-10}$	$8.5\ 10^{-10}$	3.05
10		$3.31\ 10^{-10}$	$1.2\ 10^{-10}$	$2.1\ 10^{-10}$	2.76
12	300	$2.10\ 10^{-10}$	$8.5\ 10^{-11}$	$1.9\ 10^{-10}$	2.47
14		$1.23\ 10^{-10}$	$3.8\ 10^{-11}$	$1.3\ 10^{-10}$	3.23
16		$9.20\ 10^{-11}$	$2.5\ 10^{-11}$	$1.1\ 10^{-10}$	3.68
8		$8.83\ 10^{-10}$	$2.8\ 10^{-10}$		3.15
10		$5.90\ 10^{-10}$	$1.8\ 10^{-10}$		3.27
12	350	$3.91\ 10^{-10}$	$1.4\ 10^{-10}$		2.79
14		$2.38\ 10^{-10}$	$6.7\ 10^{-11}$		3.55
16		$1.81\ 10^{-10}$	$5.1\ 10^{-11}$		3.55
8		$1.09\ 10^{-9}$	$3.9\ 10^{-10}$		2.79
10		$7.20\ 10^{-10}$	2.710^{-10}		2.66
12	400	$5.48\ 10^{-10}$	$2.3\ 10^{-10}$		2.38
14		$3.70\ 10^{-10}$	$1.2\ 10^{-10}$		3.08
16		$3.28\ 10^{-10}$	$1.05\ 10^{-10}$		3.12

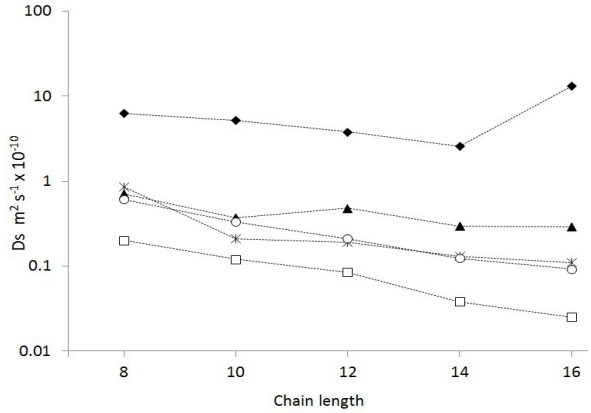

Fig 4. A plot of the calculated diffusion coefficients from the current MD simulations (o), MD simulations at infinite dilution [25] (▲), MD simulations using simpler models [19] (◆), Hierarchical simulations [18] (∗) and QENS studies [17] (□) .

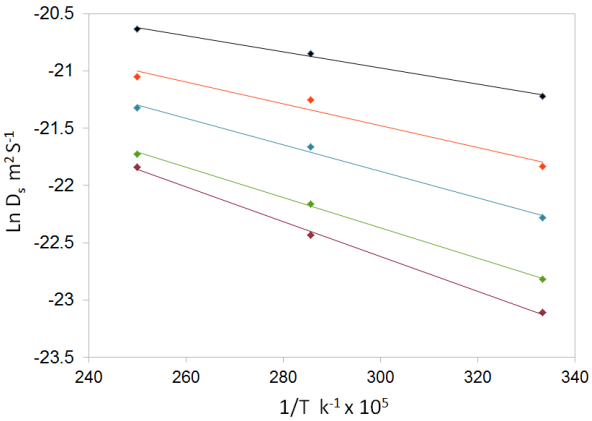

Fig 5. Arrhenius plots for C_8 (◆) C_{10}(◆) C_{12} (◆) C_{14}(◆) C_{16} (◆)

diffusion coefficients bringing them closer to those experimentally observed for these systems. From the plot in figure 4 comparing all values between the current study and those obtained at infinite dilution, one can see a significant reduction in diffusion coefficient for dodecane, tetradecane and hexadecane which are lower by a factor of 3, 3.8 and 5 respectively. However, for octane and decane, the diffusion coefficient values are still very similar to those obtained at infinite dilution.

The diffusion coefficients obtained at 300 K are also plotted in figure 4, in comparison with previous MD simulations using a united-atom model and rigid zeolite cage[19] and QENS measurements.[17] This plot clearly shows the vast improvement in accuracy of MD simulations when a more sophisticated model is used.

When the diffusion coefficients are compared with those obtained from hierarchical simulations,[18] a close agreement is shown, with almost identical values for dodecane and tetradecane, and the only significant difference occurs for decane, with a difference of a factor of 1.5. The significance of this being that the routine use

Table 3. The calculated activation energies in kJ mol^{-1} from the current MD simulations, QENS studies [17] and hierarchical simulations [18]

N	Ea (MD)	Ea (QENS)	Ea (HS)
8	5.83	7.1	4.3
10	7.77	8.6	11.2
12	9.56	10.3	11.6
14	10.40	12.3	13.1
16	12.60	15.2	11.3

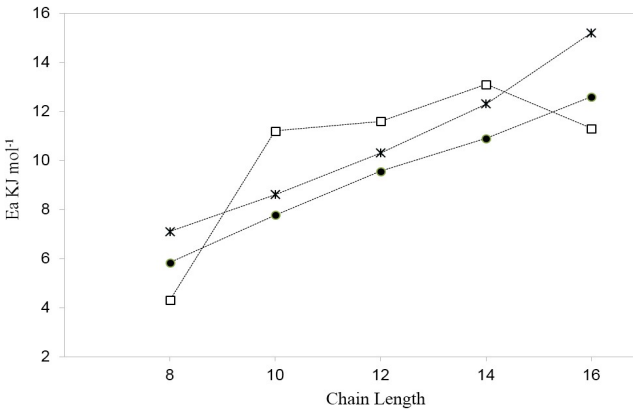

Fig 6. A plot of the activation energy of diffusion with chain length, for the current MD study (•) , QENS studies [18] (∗) and hierarchical simulations[17] (□)

of fully atomistic models for modelling diffusion behaviour in these systems is now feasible, rather than developing coarse grained models such as the referenced study. Such models will continue to be useful, but it is now clear that a full atomistic simulation is now feasible and can yield good agreement with experiment.

Notably, all the diffusion coefficients obtained by the present study are higher than those obtained experimentally, which can be attributed to the use of a perfect silicalite crystal in the simulations, allowing for faster, less hindered diffusion on the nanometre scale.

The activation energy of diffusion was calculated for each alkane using Arrhenius plots as shown in figure 5. The activation energy values obtained are tabulated and plotted in comparison with values obtained by QENS and hierarchical simulations in table 3 and figure 6 respectively. One can see that the trend (a roughly monotonic increase) of the calculated activation energies, follows that observed by QENS. In this respect the current MD simulations correlate better with experiment than the hierarchical simulations, suggesting that though the agreement in diffusion

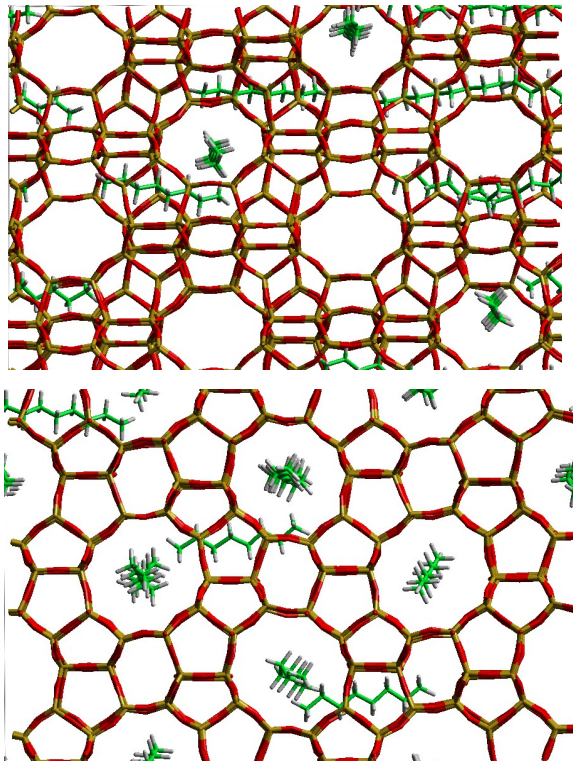

Fig 7. A snapshot of the MD simulation of *n*-octane at 400 K after 4 ns, showing that 3 octane molecules have switched from the [010] channel system to the [001] channel system.

coefficients are similar at 300 K, fully atomistic simulations show closer agreement in terms of variation in diffusion coefficient with temperature. It must be noted however, that for the current study the activation energy was calculated over the same temperature range as experiment, whereas the hierarchical simulations were calculated over a far wider temperature range.

The absolute values in activation energy show close agreement with experiment for octane, decane and dodecane (within 1.5 kJ mol^{-1}); the agreement is slightly less so for tetradecane and hexadecane with a difference of 1.9 and 2.6 kJ mol^{-1} respectively. A possible reason for this was noted in reference 30 that for longer molecules, redistribution of the molecules throughout the crystal was observed at higher temperatures. For this reason, the activation energy is observed to be higher. As these simulations are carried out using periodic boundary conditions, this behaviour is not possible due to even distribution of alkanes in the supercell being repeated infinitely. All calculated values of E_a are slightly but consistently below those obtained experimentally. This can be attributed (as with the diffusion coefficients) to the use of a perfect silicalite crystal structure, as a perfect structure would have both fewer, and lower energy barriers to diffusion than a real system containing defects,

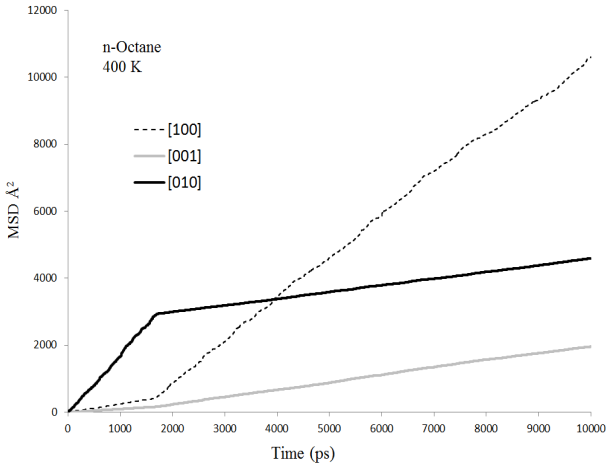

Fig 8. A plot of the mean squared displacement as a function of time for a particular channel switching *n*-octane molecule showing the change in MSD gradient in the [010] and [100] direction.

causing the variation of diffusion coefficient with temperature to decrease. Another important factor is the difficulty in identifying the activation energy for this kind of diffusion behaviour, as the jump diffusion model is no longer appropriate for the continuous Fickian diffusion observed in these simulations.

An interesting behaviour observed for octane at temperatures of 350 K and above was that of channel switching from the straight to the sinusoidal channels. This was only observed for octane, as the shorter molecular length allows it to overcome the barrier associated with switching channel systems at the junctions. There are two important factors associated with this behaviour. First, it only occurs at 350 and 400 K, so the kinetic energy supplied by this temperature increase is enough for the potential barrier at the junction to be breached. Second, the channel switch only occurs with molecules which have been placed in a channel with another octane molecule, rather than placed in the channel alone. To replicate successfully experimental loadings, 5 of the 8 available [010] channels in the supercell had 2 octane molecules inserted. It was from 3 of these 5 channels that switching was observed as illustrated in figure 7, suggesting that both the increase in temperature and the repulsion caused by sorbate-sorbate interactions between octane molecules in the same channel provide sufficient energy to breach the potential barrier associated with channel switching. This switching is illustrated also in the MSD plot in figure 8 for one octane particular molecule which showed this behaviour. The gradient in the [010] direction decreases markedly before 2 nanoseconds while the MSD gradient in the [100] direction increases, illustrating this change in diffusive direction.

Developments on this observation would involve static calculations of the energetics associated with this channel switching, so that the contributions of both the temperature and sorbate-sorbate interactions could be studied in detail, calculating precisely the magnitude of the repulsion between sorbates.

Conclusion

The diffusion coefficients and activation energies of diffusion were calculated for longer *n*-alkanes (*n*-C_8 - *n*-C_{16}) in silicalite. The measurements were carried out at temperatures of 300, 350 and 400 K at loadings matching those of previous QENS studies. The calculated diffusion coefficients were in good agreement with experimental values and were significantly better than those calculated using simpler framework and hydrocarbon models, and in the case of the longer alkanes, better agreement than those from MD studies using the same model, but without using experimental loadings. The calculated activation energies were found to give the experimentally observed monotonic increase in value, and agreed with experiment to within 1.5 kJ mol^{-1} for shorter alkanes, but with a larger difference for tetra and hexadecane, possibly due to the use of periodic boundary conditions forbidding the experimentally observed redistribution of the alkanes throughout the crystal. The calculated diffusion coefficients and activation energies were found to be in the upper limit and lower limit respectively of the experimental values which was attributed to the use of a perfect zeolite crystal for the MD studies and the breakdown of an Arrhenius relationship in the presence of continuous diffusion. Channel switching between the straight and sinusoidal channels was observed for octane at higher temperatures. This was attributed to the molecular size of octane, the kinetic energy supplied by the temperature increase, and the repulsion caused by extra octane molecules in the channel system allowing the potential barrier of channel switching at the junctions to be breached. Future work will involve static calculations of the channel switching process, and the introduction of framework aluminium and counterions to the framework, so the diffusion measurements can be compared between silicalite, and the industrially important ZSM-5. The introduction of extra-framework ions has been shown to slow the diffusion by roughly a factor of 5 for longer *n*-alkanes as expressed in reference 16 studying Na-ZSM-5, due to the potential barrier presented.

Acknowledgements

The author would like to acknowledge EPSRC, STFC and the ISIS neutron source for funding and sponsorship. J. Saβmannshausen for maintenance and use of the Faraday computer cluster, and H. Jobic for informative discussion.

References

1. J. Weitkamp, L. Puppe, L. *Catalysis and zeolites: fundamentals and applications,* Springer, 1999.
2. M. Jiang, M. Eic, S. Miachon, J. Dalmon, M. Kocirik, *Sep. Purif. Technol.,* 2001, **25,** 287–295.
3. F. Leroy, B. Rousseau, *Mol. Simul.,* 2004, **30,** 617–620.
4. R. Krishna, J.M. Van Baten, *Chem. Eng. J.,* 2008 **140,** 614–620.
5. A.O. Koriabkina, A.M. de Jong, D. Schuring, J. van Grondelle, R. A. van Santen, *J. Phys. Chem. B.,* 2002, **106,** 9559–9566.
6. D. H. Lin, V. Ducarme, G. Coudurier, J. C. Vedrine, *Stud. Surf. Sci. Catal.,* 1989, **46,** 615–623.
7. M. Yu, J. C. Wyss, R.D. Noble, J. L. Falconer, *Microporous Mesoporous Mater.,* 2008, **111,** 24–31.
8. J.R. Fried, S. Weaver, *Comput. Mater. Sci.,* 1998, **11,** 277–293.
9. F. Jianfen, B. Van de Graaf, H.M. Xiao, S.L. Njo, *J. Mol. Struct., THEOCHEM,* 1999, **492,** 133–142.
10. B. Millot, A. Méthivier, H. Jobic, H. Moueddeb, M. Bée, *J. Phys. Chem. B., 1999,* **103,** 1096–1101.
11. P. Wu, A. Debebe, Y. H. Ma, Y. *Zeolites.,* 1983, **3,** 118–122.
12. L. Song, Z. -L. Sun, L.V. Rees, *Microporous Mesoporous Mater.,* 2002, **55,** 31–49.
13. C. L. J. Cavalcante, D. M. Ruthven, *Ind. Eng. Chem. Res.,* 1995, **34,** 185–191.
14. D. Shen et al., J. Chem. Soc. Faraday Trans., 1990, **86**, 3943–3948.
15. A. Zikanova, M. Bülow, H. Schlodder, *Zeolites,* 1987, **7,** 115–118.
16. H. Jobic, J. Mol. Catal. Chem., 2000, **158,** 135–142.
17. H. Jobic, D. N. Theodorou, J. Phys. Chem. B., 2006, **110,** 1964–1967.
18. E.J. Maginn, A. T. Bell, D. N. Theodorou, J. Phys. Chem., 1996, **100**, 7155–7173.
19. R. C. Runnebaum, E. J. Maginn, *J. Phys. Chem. B.,* **101,** 1997, 6394–6408.
20. R. L. Gorring, *J. Catal.,* 1973, **31,** 13–26.
21. D. Dubbeldam, S. Calero, T. L. Maesen, B. Smit, Angew. Chem. Int. Ed., 2003, **42**, 3624–3626.
22. D. M. Ruthven, Microporous Mesoporous Mater., 2006, **96**, 262–269.
23. D. Dubbeldam, B. Smit, *J. Phys. Chem. B.,* 2003, **107,** 12138–12152.
24. E. Ruckenstein, P. S. Lee, *Phys. Lett. A.,* 1976, **56,** 423–424.
25. A. J. O'Malley, C. R. A. Catlow, *Phys. Chem. Chem. Phys.,* 2013 **15,** 19024–19030.
26. G. Artioli, C. Lamberti, G. L. Marra, *Acta Crystallogr. B.,* 2000, **56,** 2–10.
27. B. Vessal, M. Amini, C. R. A. Catlow, J. Non-Cryst. Solids., 1993, **159**, 184–186.
28. G. Herzberg, Molecular spectra and molecular structure., *N. Y. Van*

Nostrand Reinhold, 1950.
29. A. V. Kiselev, A. A. Lopatkin, A.A. Shulga, Zeolites, 1985, **5,** 261–267.
30. H. Jobic, B. Farago, *J. Chem. Phys.,* 2008 **129,** 171102–171102.
31. T. G. A. Youngs, *J. Comput. Chem.,* 2010*,* **31,** 639–648 (2010).
32. H. J. Berendsen, J. P. M. Postma, W. F. van Gunsteren, A. DiNola, J. R. Haak, *J. Chem. Phys.,* 1984*,* **81,** 3684–3690.
33. I. T. Todorov, W. Smith,, K. Trachenko, M. T. Dove, M. T. 2006 *J. Mater. Chem.,* **16,** 1911–1918.